Supporting Information

for

An Electron Acceptor Featuring B–N Covalent Bond and Small Singlet-Triplet Gap for Organic Solar Cells

Xinyuan Liu,‡[a] Shuting Pang,‡*[a] Liang Zeng,[a] Wanyuan Deng,[a] Mingqun Yang,[a] Xiyue Yuan,[a] Junyu Li,[b] Chunhui Duan,*[a] Fei Huang,[a] and Yong Cao[a]

‡ These authors contributed equally to this work.

[a] *Institute of Polymer Optoelectronic Materials and Devices*, *State Key Laboratory of Luminescent Materials and Devices*, *South China University of Technology*, *Guangzhou 510640*, *China*.

[b] *Molecular Materials and Nanosystems & Institute for Complex Molecular Systems*, *Eindhoven University of Technology*, *MB Eindhoven*, *5600*, *The Netherlands*.

E-mail: pangshuting@scut.edu.cn; duanchunhui@scut.edu.cn

1. Synthesis

General information: All the chemicals and reagents were purchased from commercial sources (Alfa Aesar and Sigma Aldrich). PM6 was synthesized according to literature.[1] The compound 1 was synthesized following our reported paper.[2] All reagents were purchased from Inno-chem, *J&K*, Sigma-Aldrich, Acros, Alfa Aesar or TCI, and used as received.

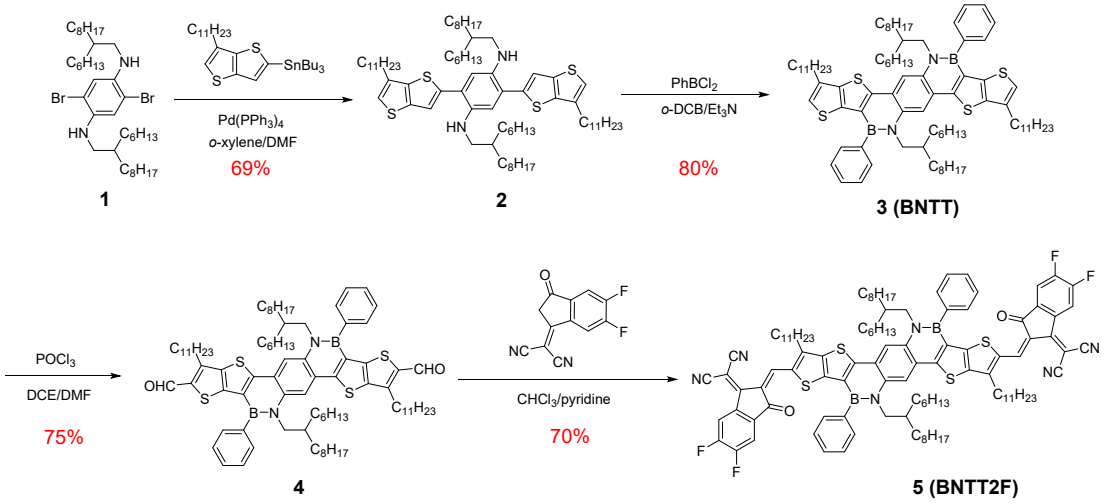

Scheme S1. The synthetic route of BNTT2F.

Synthesis of the compound 2: The compound 1 (2.9 g, 4.0 mmol) and tributyl(6-undecylthieno[3,2-b] thiophen-2-yl)stannane (2.5 g, 12.0 mmol) were dissolved in dry *o*-xylene (90 mL) in a Schlenk flask. The mixture was degassed by nitrogen for 15 minutes. $Pd(PPh_3)_4$ (0.48 g, 0.4 mmol) was added and then the mixture was heated to 140 °C and stirred overnight. Afterwards, the resulting mixture was poured into brine and extracted by dichloromethane for three times. After removing the solvent, the product was purified by silica gel column chromatography with the solvent mixture of dichloromethane/petroleum ether (1/4, v/v) as eluent, yielding a yellow oil (3.2 g, 69% yield).^{1}H NMR (500 MHz, $CDCl_3$) δ: 7.39 (s, 2H), 7.02 (s, 2H), 6.75 (s, 2H), 4.05 (br, 2H), 3.02 (m, 4H), 2.74 (t, J = 7.6 Hz, 4H), 1.77 – 1.46 (m, 12H), 1.45 – 1.05 (m, 74H), 0.97 – 0.79 (m, 18H). ^{13}C NMR (125 MHz, $CDCl_3$) δ: 205.74, 139.61, 138.77, 135.13, 132.40, 130.06, 128.26, 121.12, 118.98, 52.02, 48.63, 42.83, 39.71, 39.51, 37.54, 32.38, 31.93, 31.85, 31.65, 30.09, 30.02, 29.70, 29.66, 29.63, 29.60, 29.47, 29.24, 28.94, 28.70, 27.09, 26.72, 22.70, 14.13, 13.61.

Synthesis of the compound 3 (BNTT): To a solution of compound 2 (3.0 g, 2.6 mmol) in o-dichlorobenzene (15mL), triethylamine (2.5 g, 25 mmol) and phenyl dichloroborane (1.2 g, 7.9 mmol) were added. The mixture was degassed by nitrogen for 15 minutes, and then was heated to 180 °C for 36 hours. Afterwards, the resulting mixture was poured into brine and extracted by dichloromethane for three times. After removing the solvent, the product was purified by silica gel column chromatography with the solvent mixture of petroleum ether and dichloromethane as eluent, yielding a yellow solid (2.76 g, 80% yield). ^{1}H NMR (500 MHz, $CDCl_3$) δ: 8.24 (s, 2H), 7.63 (d, J = 7.0 Hz, 4H), 7.56 – 7.49 (m, 6H), 6.91 (s, 2H), 4.29 (d, J = 5.3 Hz, 4H), 2.78 (t, J = 7.5 Hz, 4H), 2.13 – 2.15 (m, 2H), 1.86 – 1.72 (m, 4H), 1.52 – 1.05 (m, 80H), 0.98 – 0.70 (m, 18H). ^{13}C NMR (125 MHz, $CDCl_3$) δ: 204.71, 150.98, 142.88, 139.71, 136.74, 133.43, 133.05, 131.76, 127.03, 126.77, 123.20, 121.88, 111.76, 51.53, 35.86, 30.89, 29.17, 28.92, 28.68, 28.66, 28.62, 28.48, 28.33, 27.80, 26.07, 21.66, 13.08.

Synthesis of the compound 4: To a solution of compound 3 (2 g, 1.51 mmol) in 1,2-dichloroethane (10 mL) and *N*,*N*-dimethylformamide (DMF) (12 mL) at 0 °C, phosphorous oxychloride (1.46 mL, 15.72 mmol) was added slowly under the protection of nitrogen. After stirring at 0 °C for 1 hour and then refluxed at 90 °C overnight. The reaction mixture was poured into water (150 mL) and then extracted with dichloromethane three times. The combined organic phase was washed with water, dried over Na_2SO_4, and the solvent was removed under reduced pressure. The residue was purified by silica gel column chromatograph, using petroleum ether/dichloromethane (1/1, v/v) as the eluent to give 4 as an orange oil (1.56 g, 75% yield). ^{1}H NMR (500 MHz, $CDCl_3$) δ: 9.99 (s, 2H), 8.22 (s, 2H), 7.58 (d, J = 7.0 Hz, 4H), 7.56 – 7.47 (m, 6H), 4.28 (d, J = 6.5 Hz, 4H), 3.13 (t, J = 7.3 Hz, 4H), 2.06 – 2.09 (m, 2H), 1.82 – 1.85 (m, 4H), 1.65 – 1.45 (m, 16H), 1.43 – 1.01 (m, 64H), 0.91 – 0.76 (m, 18H). ^{13}C NMR (125 MHz, $CDCl_3$) δ: 181.36, 154.61, 149.35, 146.63, 143.42, 138.18, 134.73, 133.50, 131.38, 127.45, 124.49, 122.94, 118.06, 112.50, 51.59, 35.89, 33.95, 33.85, 33.20, 30.86, 30.41, 29.29, 28.62, 28.41, 27.19, 21.64, 20.16, 13.07.

Synthesis of the compound 5 (BNTT2F): To a 100 mL two-necked flask, the compound 4 (400 mg, 0.30 mmol), 2-(5,6-difluoro-3-oxo-2,3-dihydro-1H-inden-1-ylidene)malono-nitrile (336 mg, 1.46 mmol), and dried chloroform (40 mL) were added. The mixture was degassed by nitrogen for 15 minutes. Then 0.6 mL of pyridine was added. The mixture was stirred at 65 °C for 6 hours. After

cooling to room temperature, the mixture was poured into 100 mL methanol and the precipitate was collected by filtration. The precipitate was then redissolved in chloroform and precipitated from methanol. This solubilizing-precipitating operation was repeated for three times. The final product was purified by recrystallization from chloroform/methanol, yielding a dark green solid (382 mg, 73%). ^{1}H NMR (500 MHz, $C_2D_2Cl_4$) δ: 8.84 (s, 2H), 8.39 (dd, J = 9.5, 6.4 Hz, 2H), 7.96 (s, 2H), 7.87 (d, J = 7.0 Hz, 4H), 7.81 – 7.75 (m, 6H), 7.65 (t, J = 7.6 Hz, 2H), 4.37 (d, J = 6.0 Hz, 4H), 3.28 (t, J = 7.5 Hz, 4H), 2.02 – 1.86 (m, 6H), 1.55-1.60 (m, 4H), 1.54 – 1.43 (m, 6H), 1.44 – 1.06 (m, 70H), 1.01 – 0.81 (m, 18H). ^{13}C NMR (125 MHz, $C_2D_2Cl_4$) δ: 184.16, 158.20, 157.35, 157.08, 155.05, 154.73, 152.95, 152.66, 150.17, 139.79, 138.59, 135.14, 134.69, 134.26, 132.49, 128.35, 128.26, 124.02, 120.44, 114.22, 113.86, 113.52, 112.32, 112.17, 68.34, 52.35, 36.75, 31.62, 31.41, 31.34, 31.21, 30.25, 29.78, 29.59, 29.20, 29.15, 29.11, 29.07, 28.94, 28.81, 28.72, 26.26, 22.08, 13.49. (MALDI-TOF-MS) Calcd. For $C_{110}H_{130}B_2F_4N_6O_2S_4$ (M^+): 1796.14, Found: 1796.62.

2. Measurements and characterization

Nuclear magnetic resonance (NMR): ^{1}H and ^{13}C NMR were measured on a Bruker AV-500 MHz spectrometer in $CDCl_3$ (25 °C) or $C_2D_2Cl_4$ (100 °C). Chemical shifts δ are reported in ppm using $CDCl_3$ (7.26 ppm for ^{1}H NMR and 77.0 ppm for ^{13}C NMR) or $C_2D_2Cl_4$ (5.98 ppm for ^{1}H NMR and 73.8 ppm for ^{13}C NMR) as an internal standard.

MALDI-TOF-MS: MALDI-TOF-MS was measured on Bruker Daltronik GmbH (autoflex II).

Thermogravimetric analyses (TGA): TGA were measured on NETZSCH TG 209 at a heating rate of 10 °C min^{-1} with a nitrogen flow rate of 20 mL min^{-1}.

Differential scanning calorimetry (DSC): DSC measurements were performed on a NETZSCH (DSC200F3) apparatus under a nitrogen atmosphere with a heating/cooling rate of 10/20 °C min^{-1} for the first cycle and a heating/cooling rate of 10/20 °C min^{-1} for the second cycle, respectively.

UV-vis-NIR absorption spectra: UV-vis-NIR spectra were recorded on a Shimadzu UV-3600 spectrophotometer. The solutions were prepared in chloroform with the concentration of 0.02 mg mL^{-1}. The films were prepared by spin coating the chloroform solutions onto glass substrates.

Square wave voltammetry (SWV): SWV measurements were measured on a CHI600D electrochemical workstation with Bu_4NPF_6 (0.1 M) in acetonitrile as the electrolyte. Platinum wires were used as the working and counter electrodes, and Ag/Ag^+ was used as the reference electrode. The HOMO and LUMO levels were estimated from the onset potentials by setting the oxidative peak potential of Fc/Fc^+ vs. the normal hydrogen electrode (NHE) to 0.63 V, and the NHE vs. the vacuum level to 4.5 V.[3,4]

Density functional theory (DFT) calculation: The geometry and wave function distribution were fully optimized at the B3LYP/ 6-31+G* level of theory by the absence of imaginary frequencies. The long alkyl side chains were replaced by methyl groups. All calculations were carried out with the Gaussian 09 software.[5]

Photoluminescence (PL) quenching experiments: Emission spectra were recorded on an Edinburgh Instruments FLSP920 double-monochromator spectrophotometer.

Phosphorescent emission spectra: The phosphorescent emission spectra were measured in chloroform glass matrix at 77 K using a Hitachi F-4600 fluorescence spectrometer.

Transmission electron microscope (TEM): TEM images were obtained from a JEM-2100F transmission electron microscope operated at 200 kV.

Grazing incidence wide-angle X-ray scattering (GIWAXS): 2D-GIWAXS experiments were carried out on a GANESHA 300XL+ system from JJ X-ray. The instrument is equipped with a Pilatus 300K detector, with pixel size of 172 × 172 μm. The X-ray source is a Genix 3D Microfocus Sealed Tube X-Ray Cu-source with integrated Monochromator (multilayer optic "3D version" optimized for SAXS) (30 W). The wavelength used is λ = 1.5418 Å. The detector moves in a vacuum chamber with sample-to-detector distance varied between 0.115 m and 1.47 m depending on the configuration used, as calibrated using silver behenate (d001 = 58.380 Å). The minimized background scattering plus high-performance detector allows for a detectable q-range varying from $3E^{-3}$ to 3 $Å^{-1}$ (0.2 to 210 nm). The sample was placed vertically on the goniometer and tilted to a glancing angle of 0.2° with respect to the incoming beam. A small beam was used to get a better resolution. The primary slits have a size of 0.3 (horizontal) × 0.5 mm (vertical), and the guard slits have a size of 0.1

(horizontal) × 0.3 (horizontal) mm. The accumulation time was 2 h for each measurement. In plane and out of plane line cuts were obtained using SAXSGUI program.

3. Device fabrication and characterization

Fabrication of solar cells: Patterned indium tin oxide (ITO) glass substrates were pre-cleaned sequentially by sonicating in a detergent bath, then with deionized water, acetone, and isopropanol at room temperature and in a boiled isopropanol bath, each for 10 minutes. The substrates were subjected to ultraviolet/ozone treatment at room temperature for 5 minutes. Then PEDOT:PSS (CLEVIOS^{TM} PVP AI 4083 from Heraeus) was spin-coated on the ITO glass substrates at 3000 rpm for 30 seconds to give a thickness of 40 nm, followed by baking at 150 °C for 10 minutes. The substrates were transferred to a nitrogen-filled glove box. The active layers were spin-coated on substrates at 1500-2500 rpm to give a thickness of 100 nm. Afterwards, a layer of PNDIT-F3N (10 nm) was spin-coated from a methanol solution (0.5 mg mL^{-1}) at a spin speed of 2000 rpm for 20 seconds. Finally, a layer of Ag (100 nm) was thermally evaporated at a pressure of 5×10^{-6} Torr.

Characterization of the OSCs: The photovoltaic performances of the devices were measured under AM1.5G illumination derived from a solar simulator (Enlitech, Taiwan). The current density**–**voltage (*J***–***V*) curves were recorded with a Keithley 2400 source meter. The light intensity was 100 mW cm^{-2} in the test, which was calibrated by a China General Certification Center-certified reference monocrystal silicon cell (Enlitech).

External quantum efficiencies (EQEs): The EQEs were measured on a commercial QE measurement system (QE-R3011, Enlitech). The light intensity at each wavelength was calibrated by a standard single-crystal Si photovoltaic cell.

Light-intensity dependence measurements: For light-intensity dependence measurements, the cell was fixed behind an aperture (radius = 1 mm) in a nitrogen-filled container with a quartz window. A green LED (Thor Labs M530L3, 530 nm) was driven at 1**–**1000 mA. The short-circuit current generated by the test cell was measured with Keithley 2400. The photon flux at each LED-current was calculated using the calibrated silicon reference.

Fabrication and characterization of single-carrier devices: Single-carrier devices were fabricated to measure hole and electron mobility by using the space-charge-limited current (SCLC) method. The device structures of the hole-only and electron-only devices are ITO/PEDOT:PSS (40 nm)/active layer (100 nm)/MoO_x (10 nm)/Ag (100 nm) and ITO/ZnO (40 nm)/active layer (100 nm)/PFN-Br (10 nm)/Ag (100 nm), respectively. The dark current densities of the blends were measured by applying a voltage between 0 and ±5 V using a computer-controlled Keithley 2400 source meter under an N_2 atmosphere. The data were analyzed according to the Mott–Gurney law that considers a Poole–Frenkel-type dependence of mobility on the electric field, given by $J = \frac{9}{8}\varepsilon_r\varepsilon_0\mu_0\frac{V^2}{d^3}\exp(0.89\gamma\sqrt{V/d})$, where ε_0 is the permittivity of free space, ε_r is the dielectric constant of the polymer which is assumed to be 3 for organic semiconductors, μ_0 is the zero-field mobility, V is the voltage drop across the device, d is the film thickness of the active layer, and γ is a parameter that describes the strength of the field-dependence effect. The applied voltage is used without correcting for series resistance or built-in voltage, which offers the best fitting of the experimental data following the protocol reported in the literature.[6] The hole and electron mobilities are extracted with the fit parameters at an electric field (E) of 1×10^5 V cm^{-1} by the Murgatroyd equation $\mu = \mu_0\exp(\gamma\sqrt{E})$.

EL measurements: The electroluminescence spectra were acquired by a high-sensitivity spectrometer (QE Pro and NIR Quest 512, Ocean Optics), while the external quantum efficiency of EL was determined by measuring the emitted photons in all direction through an integrated sphere by using a calibrated spectrometer (QE Pro, Ocean Optics), with the device injected by an external current/voltage source with constant current density.

4. Additional figures and tables

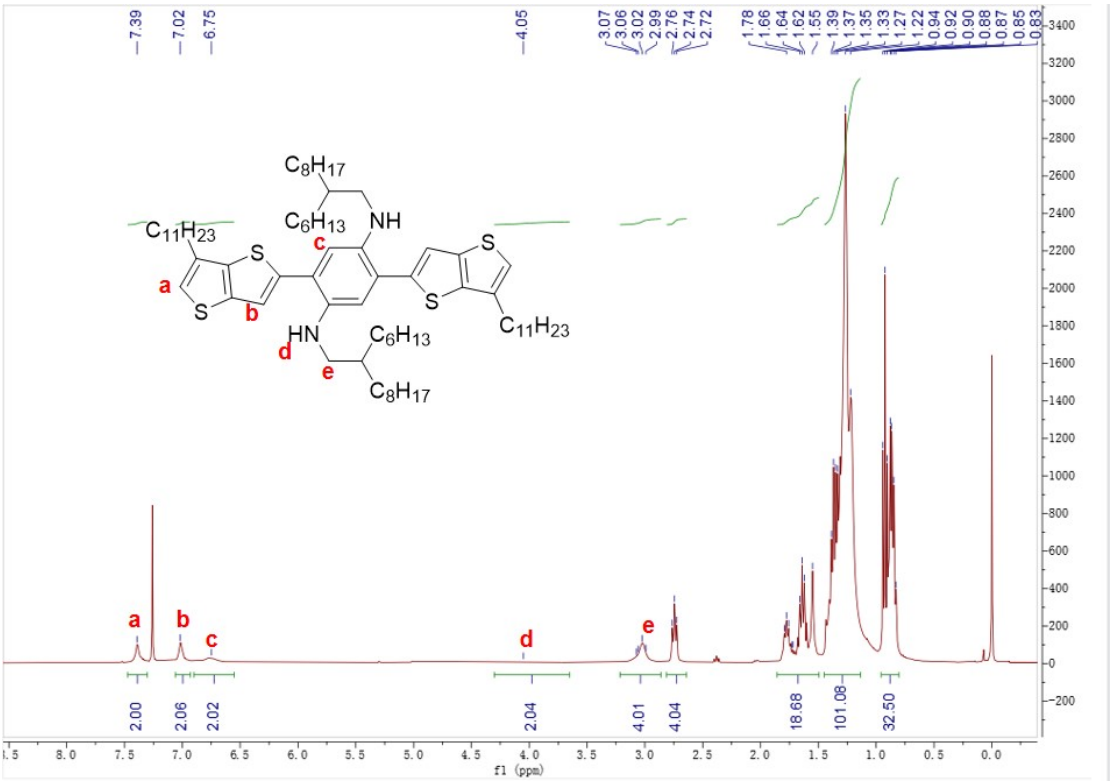

Fig. S1. ^{1}H NMR spectrum of the compound 2.

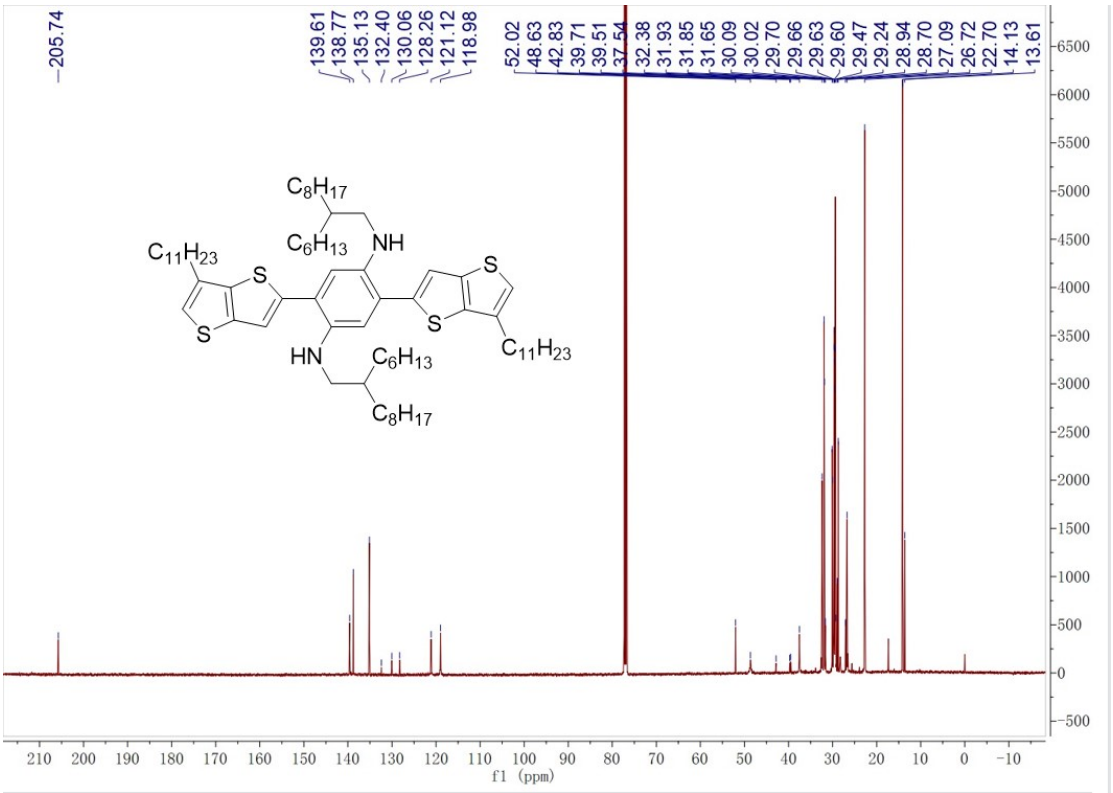

Fig. S2. ^{13}C NMR spectrum of the compound 2.

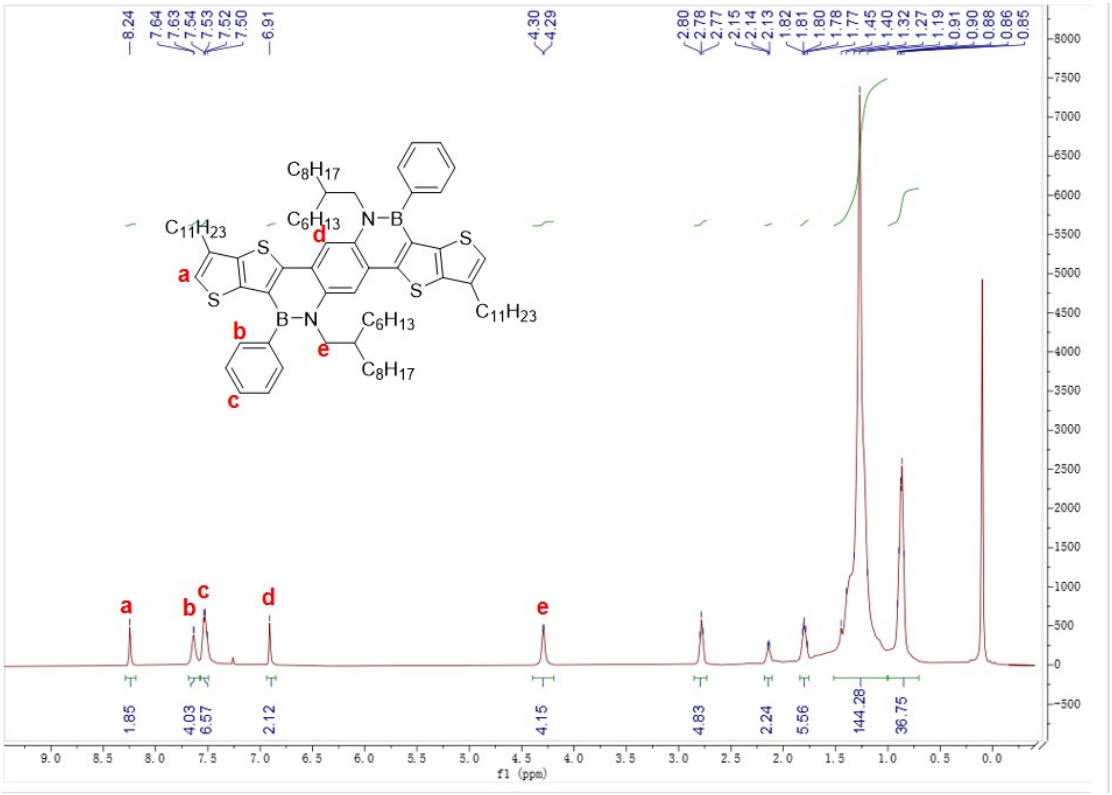

Fig. S3. ^{1}H NMR spectrum of the compound 3.

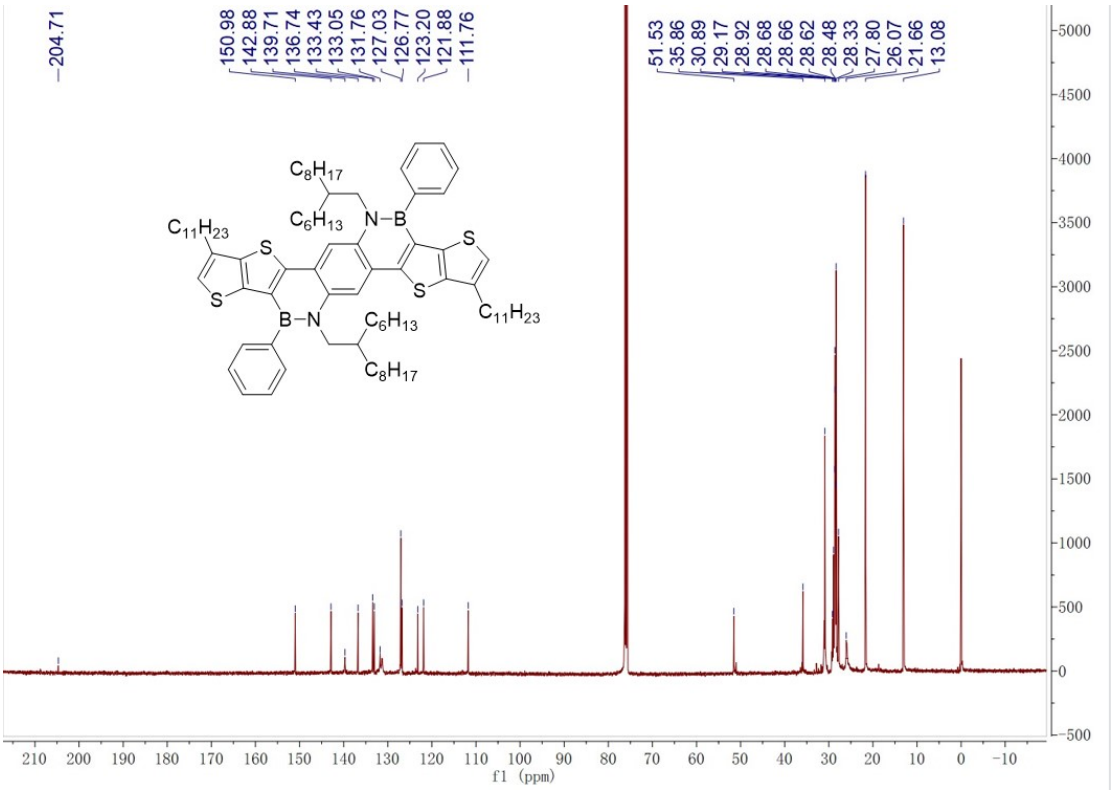

Fig. S4. ^{13}C NMR spectrum of the compound 3.

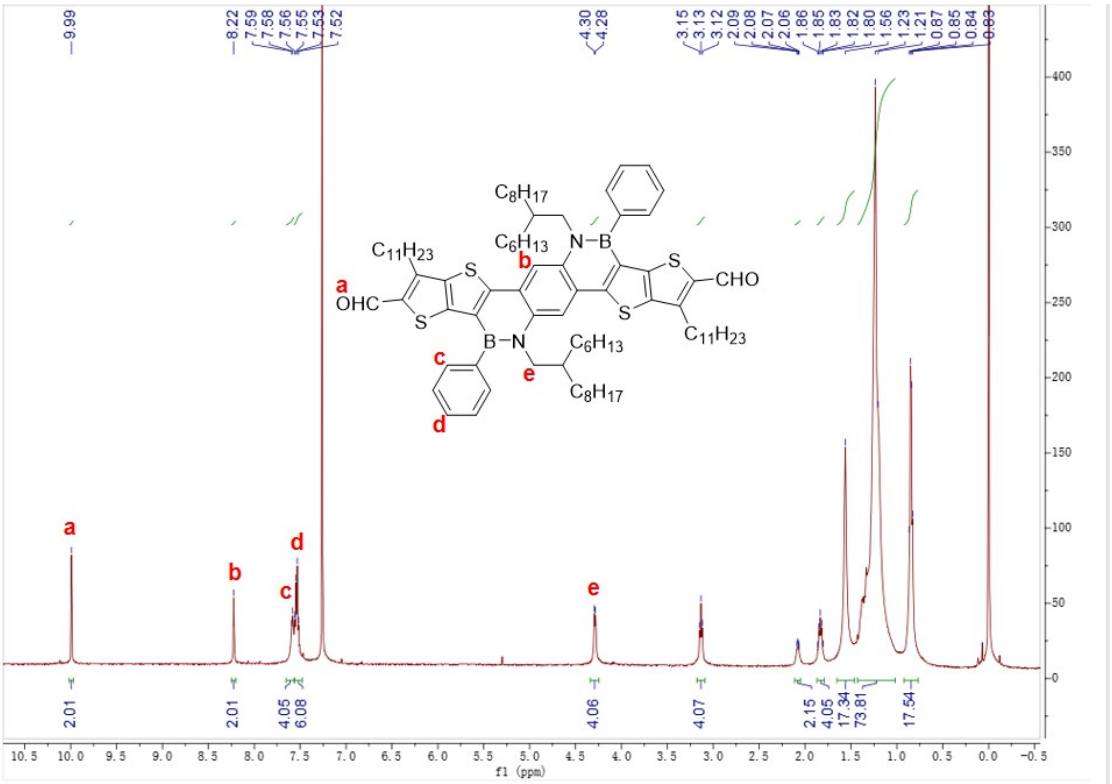

Fig. S5. ^{1}H NMR spectrum of the compound 4.

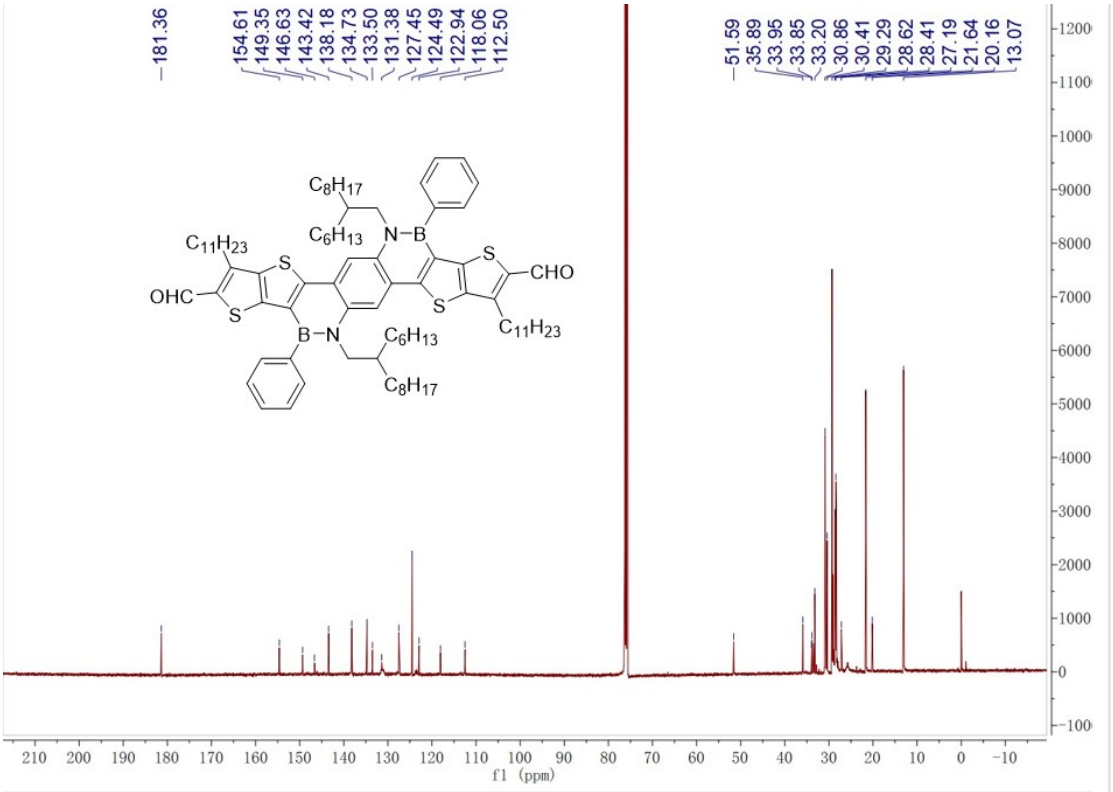

Fig. S6. ^{13}C NMR spectrum of the compound 4.

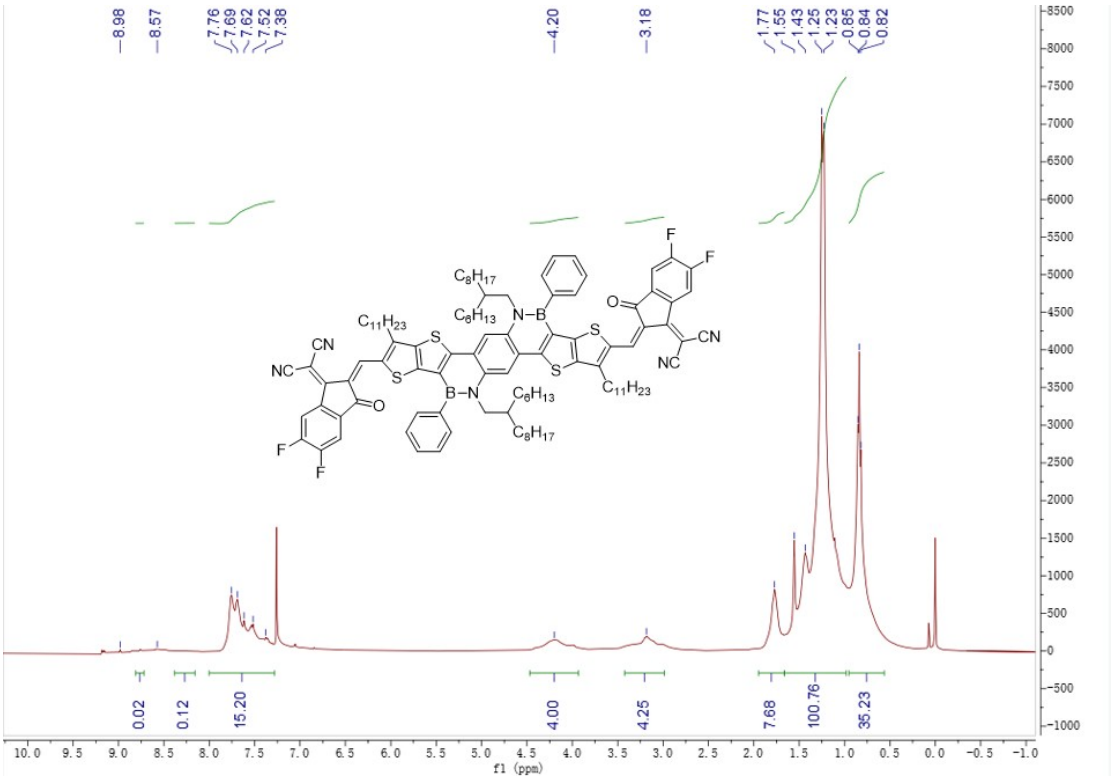

Fig. S7. ^{1}H NMR spectrum of BNTT2F in $CDCl_3$ at room temperature.

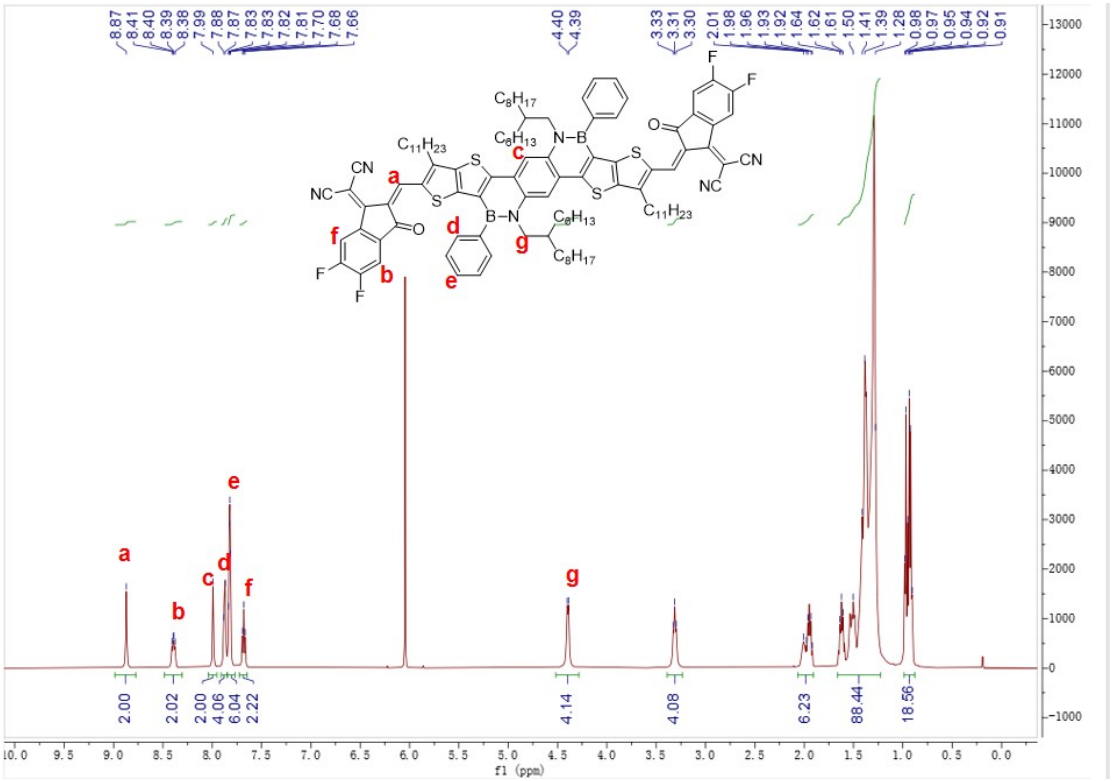

Fig. S8. ^{1}H NMR spectrum of BNTT2F in $C_2D_2Cl_4$ at 100 °C.

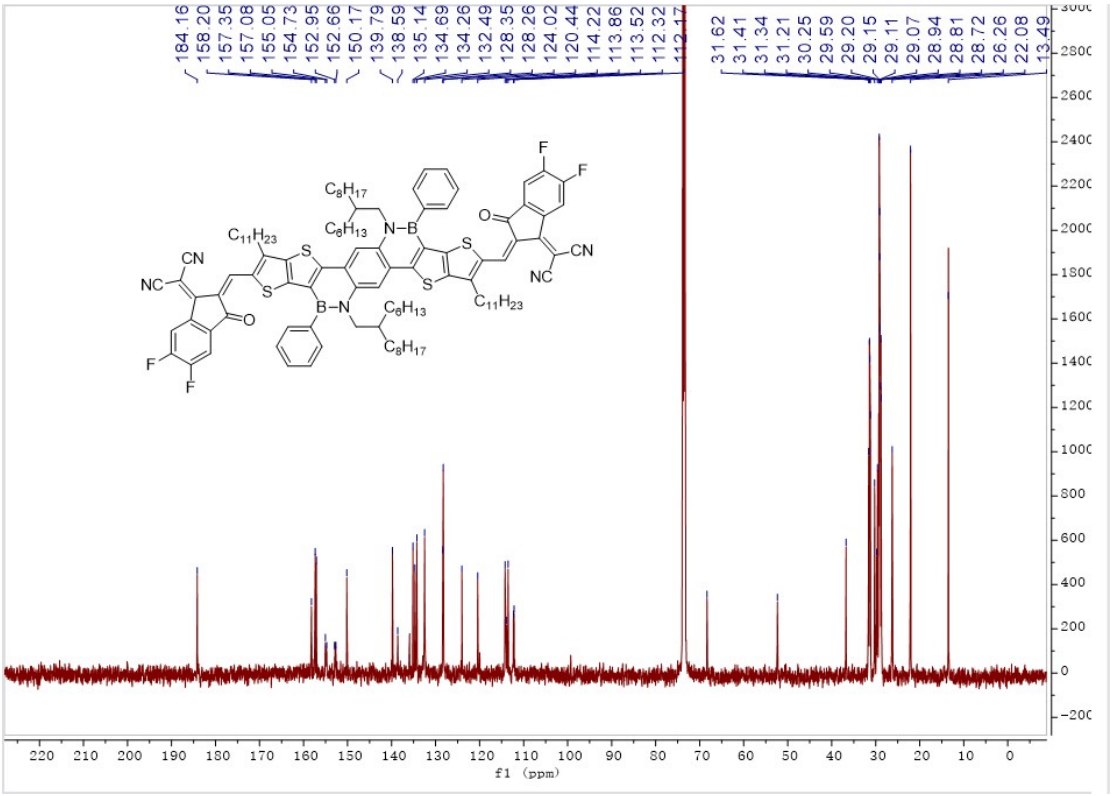

Fig. S9. ^{13}C NMR spectrum of BNTT2F in $C_2D_2Cl_4$ at 100 °C.

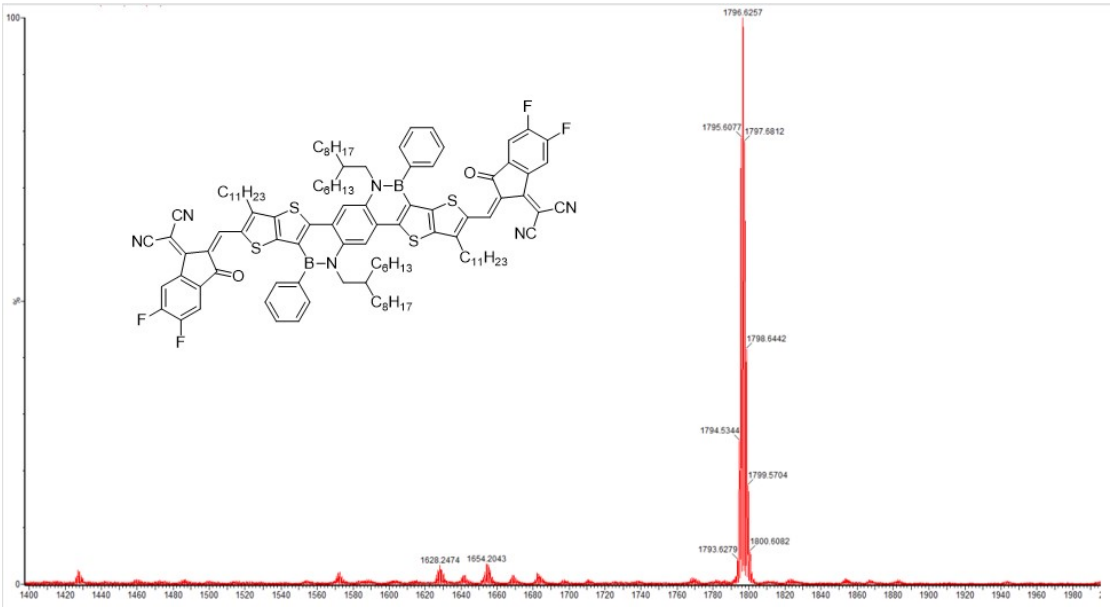

Fig. S10. MALDI-TOF of BNTT2F.

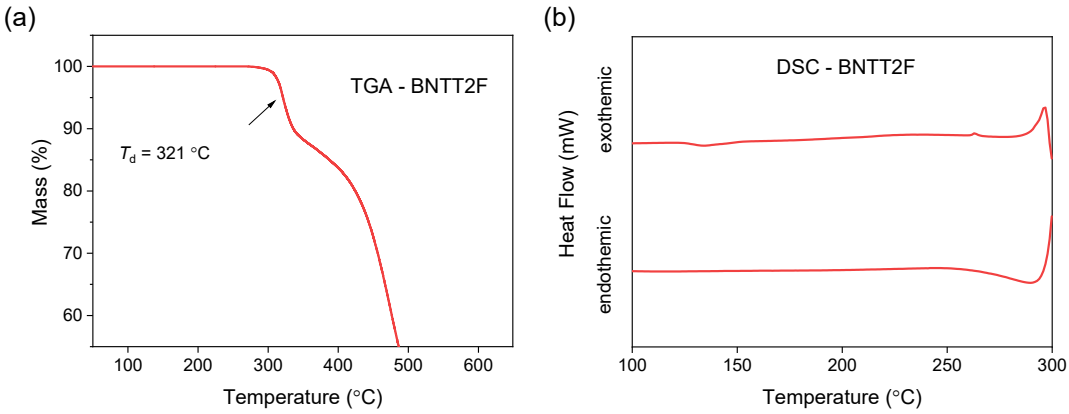

Fig. S11. (a) TGA plot of BNTT2F with a heating rate of 10 °C min^{-1} under nitrogen atmosphere; (b) the second cycle of the DSC traces of BNTT2F with a heating rate of 10 °C min^{-1} and cooling rate of 20 °C min^{-1}.

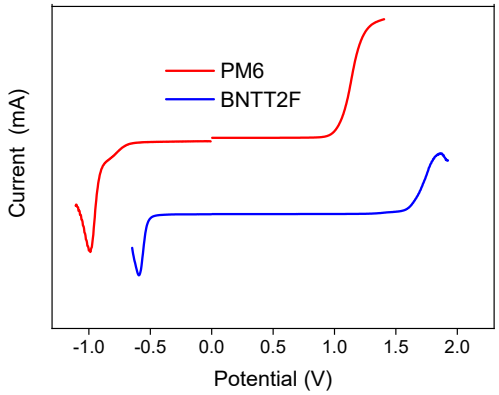

Fig. S12. Square wave voltammograms of BNTT2F and PM6.

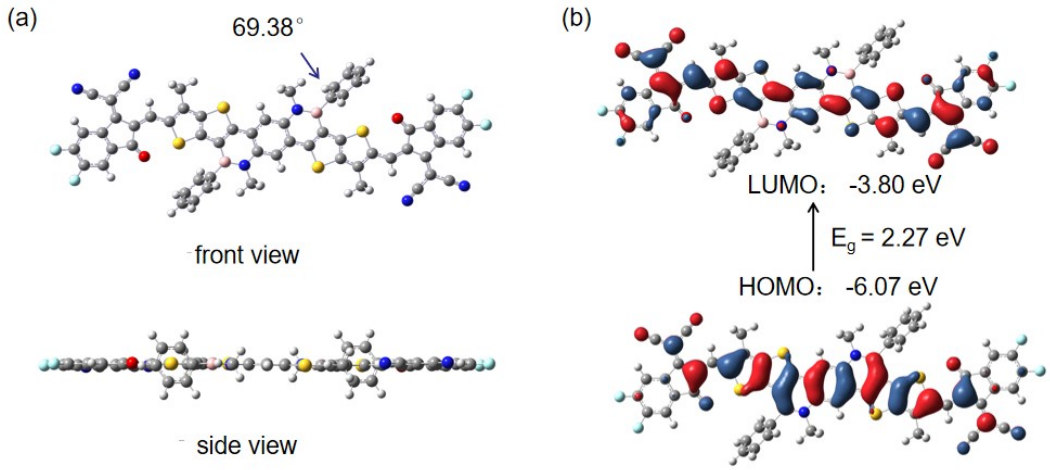

Fig. S13. (a) Front-view and side-view of optimized geometry and (b) wave function distribution of frontier molecular orbitals and energy levels of BNTT2F simulated by DFT calculation. The long alkyl chains of BNTT2F were replaced by methyl to simplify the calculations.

Table S1. Device metrics of the OSCs based on PM6:BNTT2F blends under AM1.5G irradiation (100 mW cm^{-2}).

D/A	Solvent [a]	TA	V_{oc} (V)	J_{sc} (mA cm^{-2})	FF (%)	PCE (%)
1:2	CF	None	1.00	10.7	46.3	5.0
1:2.5			1.00	10.9	46.8	5.1
1:3			0.99	10.1	45.0	4.5
1:2.5	CF+0.25% DPE	None	0.99	8.2	40.2	3.3
	CF+0.25% DIO	None	0.99	12.5	48.4	6.0
	CF+0.25% ODT	None	0.98	12.9	51.9	6.6
		None	1.00	13.3	51.2	6.8
		None	0.98	12.5	49.1	6.0
		80 °C, 10 min	0.99	13.8	60.6	8.3
		100 °C, 10 min	0.94	13.2	58.2	7.2
		120 °C, 10 min	0.91	11.6	51.2	5.4

[a] DPE is diphenyl ether, DIO is 1,8-diiodooctane.

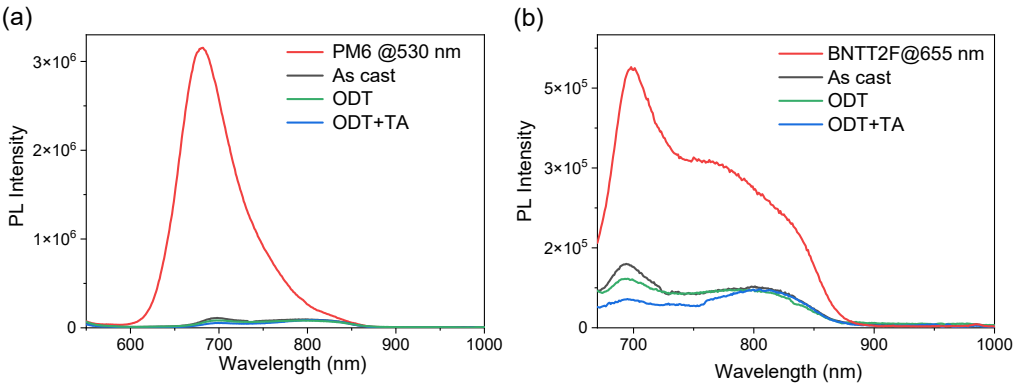

Fig. S14. The photoluminescence spectra of (a) PM6 and PM6:BNTT2F blend films excitated at 530 nm; (b) BNTT2F and PM6:BNTT2F blend films excitated at 655 nm.

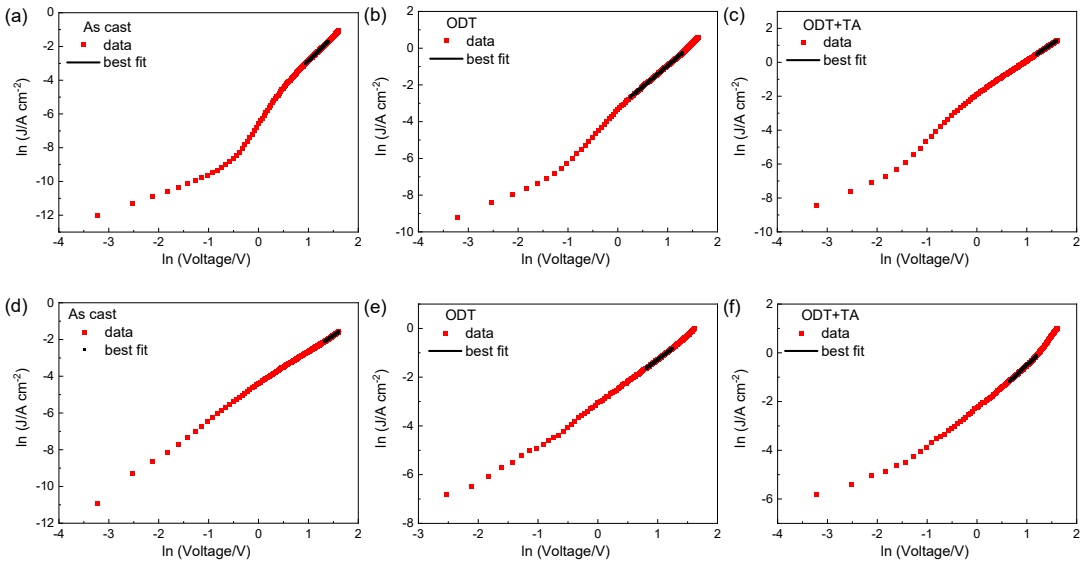

Fig. S15. (a-c) The *J*–*V* characteristics of the electron-only devices of ITO/ZnO/PM6:BNTT2F/PFN-Br/Ag; (d-f) the *J*–*V* characteristics of the hole-only devices of ITO/PEDOT:PSS/PM6:BNTT2F/MoO_x/Ag.

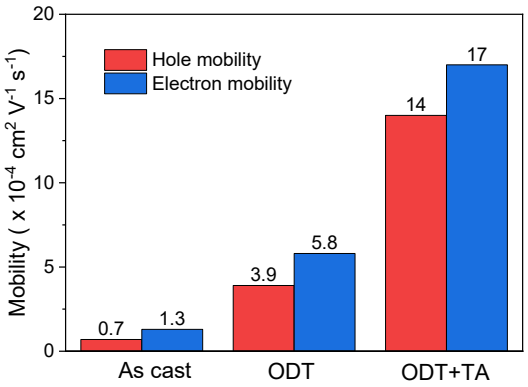

Fig. S16. Electron and hole mobilities of the PM6:BNTT2F blend films under different processing conditions (as cast, ODT, and ODT+TA).

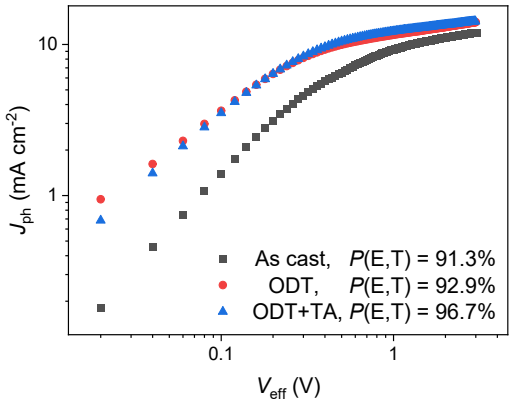

Fig. S17. Photocurrent versus effective voltage of the OSCs based on PM6:BNTT2F blends under different processing conditions (as cast, ODT, and ODT+TA).

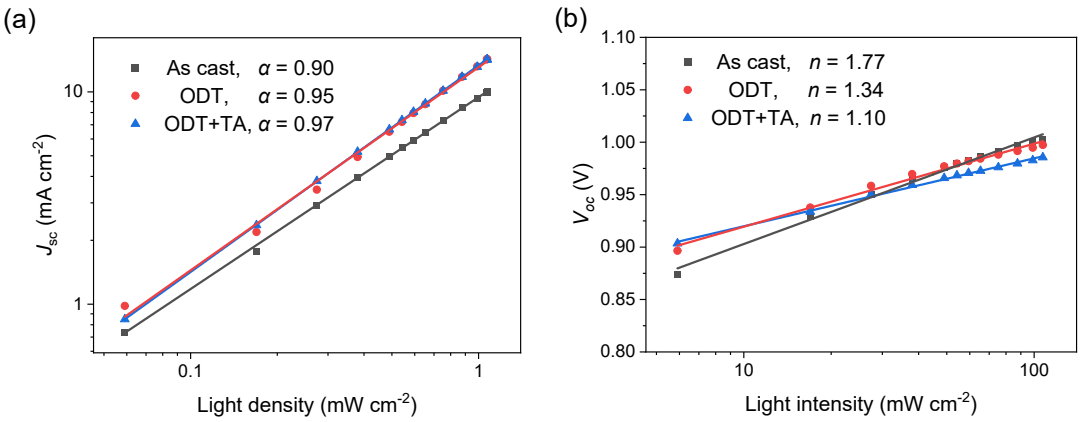

Fig. S18. (a) J_{sc} and (b) V_{oc} versus light intensity of the OSCs based on PM6:BNTT2F blends under different processing conditions (as cast, ODT, and ODT+TA).

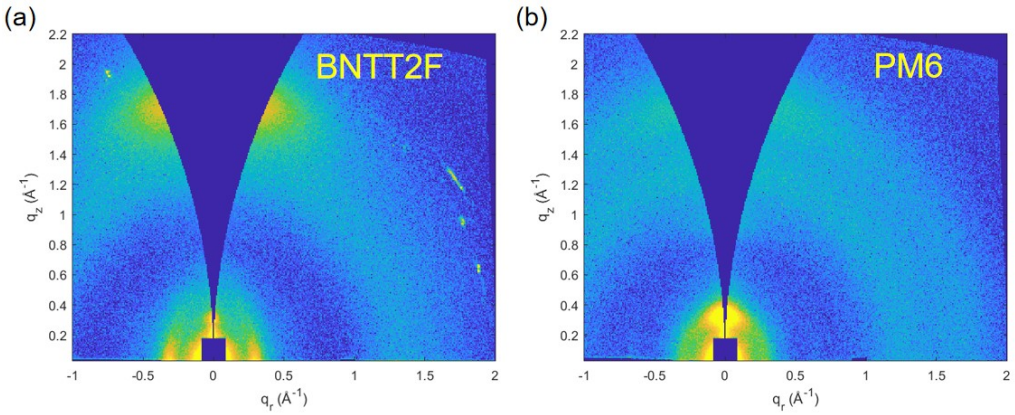

Fig. S19. 2D-GIWAXS patterns of the neat PM6 and BNTT2F films.

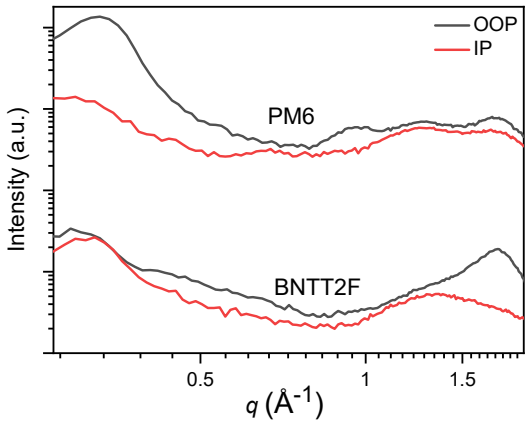

Fig. S20. 1D-GIWAXS line-cut profiles of neat PM6 and BNTT2F films.

Table S2. Characteristic length scale of the neat PM6 and BNTT2F films measured by GIWAXS.

Film	π-π stacking (010)			Lamellar stacking (100)		
	q (Å^{-1})	*d*-spacing	CCL	*q* (Å^{-1})	*d*-spacing	CCL
PM6	1.70	3.70	14.14	0.28	22.44	42.84
BNTT2F	1.73	3.63	28.27	0.31	20.27	56.25

Table S3. Characteristic length scale of the PM6:BNTT2F blend films measured by GIWAXS.

Film	π-π stacking (010)			Lamellar stacking (100)		
	q (Å^{-1})	*d*-spacing	CCL	*q* (Å^{-1})	*d*-spacing	CCL
As cast	1.73	3.63	17.67	0.31	20.27	74.55
ODT	1.73	3.63	20.94	0.31	20.27	82.54
ODT+TA	1.73	3.63	21.75	0.31	20.27	84.59

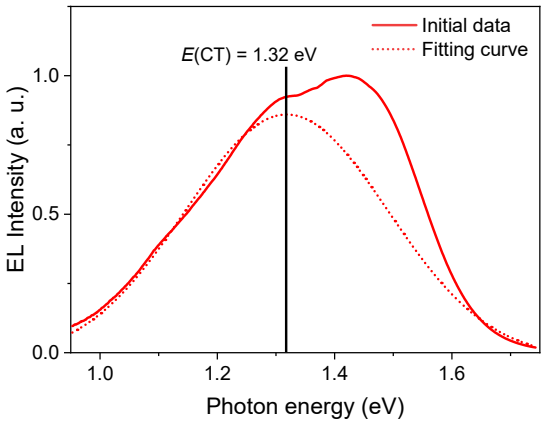

Fig. S21. EL spectrum of the OSC based on PM6:BNTT2F.

References

[1] M. Zhang, X. Guo, W. Ma, H. Ade and J. Hou, *Adv*. *Mater*., 2015, **27**, 4655.

[2] S. Pang, Z. Wang, X. Yuan, L. Pan, W. Deng, H. Tang, H. Wu, S. Chen, C. Duan, F. Huang and Y. Cao, *Angew*. *Chem*. *Int*. *Ed*., 2021, **60**, 8813.

[3] V. Pavlishchuk and A. W. Addison, *Inorg*. *Chim*. *Acta*., 2000, **298**, 97.

[4] A. J. Bard and L. R. Faulkner, *Electrochemical Methods: Fundamentals and Applications*, Wiley, 2000.

[5] M. J. Frisch, G. W. Trucks, H. B. Schlegel, G. E. Scuseria, M. A. Robb, J. R. Cheeseman, G. Scalmani, V. Barone,B. Mennucci, G. A. Petersson, H. Nakatsuji, M. Caricato, X. Li, H. P. Hratchian, A. F. Izmaylov, J. Bloino, G. Zheng, J. L. Sonnenberg, M. Hada, M. Ehara, K. Toyota, R. Fukuda, J. Hasegawa, M. Ishida, T. Nakajima, Y. Honda, O. Kitao, H. Nakai, T. Vreven, J. A. Montgomery, J. E. Peralta, F. Ogliaro, M. Bearpark, J. J. Heyd, E. Brothers, K. N. Kudin, V. N. Staroverov, R. Kobayashi,

J. Normand, K. Raghavachari, A. Rendell, J. C. Burant, S. S. Iyengar, J. Tomasi, M. Cossi, N. Rega, J. M. Millam, M. Klene, J. E. Knox, J. B. Cross, V. Bakken, C. Adamo, J. Jaramillo, R. Gomperts, R. E. Stratmann, O. Yazyev, A. J. Austin, R. Cammi, C. Pomelli, J. W. Ochterski, R. L. Martin, K. Morokuma, V. G. Zakrzewski, G. A. Voth, P. Salvador, J. J. Dannenberg, S. Dapprich, A. D. Daniels, O. Farkas, J. B. Foresman, J. V. Ortiz, J. Cioslowski and D. J. Fox, *Gaussian-09*, *Revision A.02*, Wallingford CT.

[6] J. C. Blakesley, F. A. Castro, W. Kylberg, G. F.A. Dibb, C. Arantes, R. Valaski, M. Cremona, J. S. Kim and J. Kim, *Org*. *Electron*., 2014, **15**, 1263.